Feed-back loops integrating RELA, SOX18 and FAK mediate the break-down of the lymph-endothelial barrier that is triggered by 12(S)-HETE

STEFANIE ENGLEITNER[1], DANIELA MILOVANOVIC[1], KERSTIN KIRISITS[1], STEFAN BRENNER[2], JUNLI HONG[1,3], NATHALIE ROPEK[4], NICOLE HUTTARY[1], JUDITH REHAK[1], CHI HUU NGUYEN[1,2,5], ZSUZSANNA BAGO-HORVATH[1], SIEGFRIED KNASMÜLLER[4], RAINER DE MARTIN[6], WALTER JÄGER[2] and GEORG KRUPITZA[1]

[1]Department of Pathology, Medical University of Vienna; [2]Department of Clinical Pharmacy and Diagnostics, Faculty of Life Sciences, University of Vienna, A-1090 Vienna, Austria; [3]School of Pharmacy, Nanjing Medical University, Nanjing 211166, P.R. China; [4]Institute of Cancer Research, Department of Internal Medicine 1, Medical University of Vienna; [5]Department of Internal Medicine 1, Medical University of Vienna; [6]Department of Vascular Biology and Thrombosis Research, Centre of Biomolecular Medicine and Pharmacology, Medical University of Vienna, A-1090 Vienna, Austria

Received July 30, 2019; Accepted January 24, 2020

DOI: 10.3892/ijo.2020.4985

Abstract. Metastatic cancer cells cross endothelial barriers and travel through the blood or lymphatic fluid to pre-metastatic niches, leading to their colonisation. 'S' stereoisomer 12S-hydroxy-5Z,8Z,10E,14Z-eicosatetraenoic acid [12(S)-HETE] is secreted by a variety of cancer cell types and has been indicated to open up these barriers. In the present study, another aspect of the endothelial unlocking mechanism was elucidated. This was achieved by investigating 12(S)-HETE-treated lymph endothelial cells (LECs) with regard to their expression and mutual interaction with v-rel avian reticuloendotheliosis viral oncogene homolog A (RELA), intercellular adhesion molecule 1, SRY-box transcription factor 18 (SOX18), prospero homeobox 1 (PROX1) and focal adhesion kinase (FAK). These key players of LEC retraction, which is a prerequisite for cancer cell transit into vasculature, were analysed using western blot analysis, reverse transcription-quantitative PCR and transfection with small interfering (si)RNA. The silencing of a combination of these signalling and executing molecules using siRNA, or pharmacological inhibition with defactinib and Bay11-7082, extended the mono-culture experiments to co-culture settings using HCT116 colon cancer cell spheroids that were placed on top of LEC monolayers to measure their retraction using the validated 'circular chemorepellent-induced defect' assay. 12(S)-HETE was indicated to induce the upregulation of the RELA/SOX18 feedback loop causing the subsequent phosphorylation of FAK, which fed back to RELA/SOX18. Therefore, 12(S)-HETE was demonstrated to be associated with circuits involving RELA, SOX18 and FAK, which transduced signals causing the retraction of LECs. The FAK-inhibitor defactinib and the NF-κB inhibitor Bay11-7082 attenuated LEC retraction additively, which was similar to the suppression of FAK and PROX1 (the target of SOX18) by the transfection of respective siRNAs. FAK is an effector molecule at the distal end of a pro-metastatic signalling cascade. Therefore, targeting the endothelial-specific activity of FAK through the pathway demonstrated herein may provide a potential therapeutic method to combat cancer dissemination via vascular routes.

Correspondence to: Dr Georg Krupitza, Department of Pathology, Medical University of Vienna, Waehringer Guertel 18-20, A-1090 Vienna, Austria
E-mail: georg.krupitza@meduniwien.ac.at

Abbreviations: 12(S)-HETE, 12S-hydroxy-5Z,8Z,10E,14Z-eicosatetraenoic acid, 'S' stereoisomer; 12-HETER, 12(S)-HETE receptor (syn. GPR31); BLT2, Leukotriene B4 receptor 2 (syn. BLT2 receptor, BLT2R, low affinity LTB4 receptor); CCID, Circular chemorepellent induced defect; CYP1A1, Cytochrome P450 1A1; FAK, Focal adhesion kinase; ICAM-1, Intercellular adhesion molecule 1; IKK1, IκB kinase 1 (also IKK-α); PMN, pre-metastatic niche; PROX1, Prospero homeobox protein 1; RELA, V-Rel avian reticuloendotheliosis viral oncogene homolog A; SOX18, SRY-related HMG-box 18

Key words: endothelial retraction, SRY-related HMG-box 18, V-Rel avian reticuloendotheliosis viral oncogene homolog A, focal adhesion kinase, feed-back loop

Introduction

The outgrowth of malignant tumour cells along vascular routes facilitates their dissemination to distant organs, leading to further colonization (1-3). An early step of this multistep process is the destabilisation of the endothelial barrier as a prerequisite for the cancer cell invasion into and leakage

out of lymphatic or blood vessels (intra- and extravasation, respectively) (4). The disintegration of the endothelium is induced by metabolites or polypeptides (5,6), which are secreted by a variety of tumour cell types. The present study focussed on a mechanism triggered by 'S' stereoisomer 12S-hydroxy-5Z,8Z,10E,14Z-eicosatetraenoic acid [12(S)-HETE], which serves an important role in making the lymphatic wall accessible (7). 12(S)-HETE causes loss of vascular resilience due to the retraction of endothelial cells (ECs) (8), resulting in the formation of gaps in the endothelial layer, known as 'circular chemorepellent-induced defects' (CCIDs), through which cancer cells cross the endothelial wall and subsequently spread to the lymph nodes (7). Under physiological conditions, neutrophils traverse vessel barriers by similar or lipoxin-induced mechanisms and reach sites of inflamed tissue (9). Cancer cells seem to re-activate processes, including 12(S)-HETE secretion, which enable their movement through the vasculature and foreign tissues and are otherwise used by neutrophils during the immune response (9).

12(S)-HETE triggers signalling through high- and low-affinity receptors, including 12-HETER and leukotriene B4 receptor 2 (BLT2), respectively. Subsequently, phospholipase C, Ca^{2+}-release and CAM-kinase, as well as RHO, RAK and myosin light chain kinase (MYLK), are actively phosphorylated and induce the target of MYLK, myosin light chain 2 (MLC2). This causes lymph EC (LEC) retraction and therefore the breakdown of the endothelial barrier and CCID formation (10,11). Furthermore, focal adhesion kinase (FAK), which is a non-receptor tyrosine kinase that is required for cell-matrix contact, migration and cell signalling, was demonstrated to contribute to this phenomenon (12). However, how FAK is associated in the signal transduction network triggering LEC retraction, and whether FAK is regulated by 12(S)-HETE is yet to be determined. There is a cross-talk between FAK and NF-κB (13,14), and NF-κB has been reported to regulate the endothelial lineage-determining transcription factor SRY-box transcription factor 18 (SOX18), which supports endothelial cell differentiation during embryonic development (15,16), in human umbilical vein ECs (17) and LECs (18). A previous study demonstrated that SOX18, and its transcriptional target the lymph endothelial transcription factor and marker protein prospero homeobox 1 (PROX1), contributed to CCID formation in the lymph-endothelial barrier (18). The transcription factor NF-κB and its transcriptional target, the intercellular adhesion molecule 1 (ICAM-1), were also revealed to be required for CCID formation (6,19,20). ICAM-1 is an effector necessary for cell-cell adhesion (20) and FAK is not only a signal transducer but also an effector molecule regulating cell adherence and migration (12), and both ICAM-1 and FAK are obligatory for the retraction of LECs (12,20). The retraction of LECs can be studied in a co-culture assay consisting of LEC monolayers and tumour spheroids (5,7,12), such as 12(S)-HETE-secreting HCT116 colon cancer cell spheroids, which are placed on top of LECs. This assay monitors the formation of CCIDs in the LEC monolayer underneath tumour emboli (7,19).

The elucidation of the mechanism that unlocks the lymph-endothelial barrier, which is partly mediated by the endothelial-specific transcription factors SOX18 and PROX1, may allow the targeting and inhibition of an early metastatic step with high accuracy and few side effects. Therefore, the present study investigated whether v-rel avian reticuloendotheliosis viral oncogene homolog A (RELA; the major component of the NF-κB heterodimer), SOX18 and FAK are interconnected in a common signal transduction pathway upon stimulation of LECs with 12(S)-HETE.

Materials and methods

Antibodies and reagents. Rabbit polyclonal antibodies against focal adhesion kinase (FAK; 1:1,000; cat. no. 3285), phospho-Tyr397-FAK (pFAK; 1:1,000; cat. no. 3283) and mouse monoclonal anti-v-Rel avian reticuloendotheliosis viral oncogene homolog A antibody (RELA/p65 clone L8F6; 1:1,000; cat. no. 6956) were purchased from Cell Signalling Technology Inc. and mouse monoclonal anti-β-actin antibody (clone AC-15; 1:5,000; cat. no. A3854) was purchased from Sigma-Aldrich; Merck KGaA. Rabbit polyclonal anti-SRY-related HMG-box 18 (SOX18; 1:600, cat. no. TA324592) was purchased OriGene Technologies, Inc. and rabbit monoclonal anti-prospero homeobox 1 antibody (PROX1 clone EPR19273; 1:500; cat. no. Ab119359) and mouse monoclonal anti-intercellular adhesion molecule 1 antibody (ICAM-1; 1:1,000; clone MEM111; cat. no. Ab2213) were purchased from Abcam. HRP-conjugated swine anti-rabbit antibody (1:5,000; cat. no. P0217) and HRP-conjugated rabbit anti-mouse (1:10,000; cat. no. P0260) were purchased from Dako; Agilent Technologies, Inc.

siRNAs were used for transfection of LECs, which were subsequently analyzed using western blot analysis, qPCR and in CCID assay. siRNAs against RELA (siRELA; cat. no. s11914), PTK-2 (siFAK; cat. no. s11485), ICAM-1 (siICAM-1; cat. no. s7087) and Silencer Select Negative Control SilencerR No. 1 si-RNA (n.t.Co; cat. no. 4390843) were purchased from Ambion; Thermo Fisher Scientific, Inc, and SOX18 (siSOX18; cat. no. L-019035-00-0005) and PROX1 (siPROX1; cat. no. L-016913-005) were purchased from GE Healthcare Dharmacon, Inc.

qPCR primers were used to quantify mRNA expression in LECs upon transfection of siRNAs and treatment with 12(S)-HETE. Q-PCR primers for SOX18 (cat. no. Hs00746079_s1), RELA (cat. no. Hs00153294_m1), ICAM-1 (cat. no. Hs00164932_m1), PROX1 (cat. no. Hs00896294_m1) and β-actin (cat. no. Hs01060665_g1) were purchased from TaqMan (Applied Biosystems; Thermo Fisher Scientific, Inc.).

12(S)-HETE (CAS: 54397-83-0) was purchased from Enzo Life Sciences (cat. no. BML-H012-0050), Bay11-7082 (cat. no. 196870) from EMD Millipore, parthenolide (cat. no. P0667), arachidonic acid (cat. no. 10931), proadifen hydrochloride (cat. no. P1061), guanfacine (cat. no. G1041), vinpocetine (cat. no. V6382) and curcumin (cat. no. 08511) were purchased from Sigma-Aldrich; Merck KGaA, and defactinib (cat. no. S7654; VS-6063 and PF-04554878) from Selleck Chemicals.

Cell lines. HCT 116 colon cancer cells (cat. no. 91091005) were purchased from the European Collection of Authenticated Cell Cultures (ECACC) by Public Health England and cultured at 37˚C in MEM medium (Gibco; Invitrogen; Thermo Fisher Scientific, Inc.) supplemented with 10% foetal calf serum (FCS; Gibco; Invitrogen; Thermo Fisher Scientific, Inc.),

1% penicillin/streptomycin (PS) and 1% non-essential amino acids (Gibco; Invitrogen; Thermo Fisher Scientific, Inc.). Human micro-vessel endothelial cells were purchased from Clonetics™ (Lonza Group, Ltd.). According to the protocols of previous studies and following stable transfection with telomerase, lymph endothelial cells (LECs) were isolated from this immortalised mixture of human dermal endothelial cells (21,22). LECs were grown at 37˚C in EGM-2MV (EBM2-based medium CC3156 and supplement CC4147; Lonza Group Ltd.). Cells were kept at 37˚C in a humidified atmosphere containing 5% CO_2 for subsequent experimentation.

SiRNA transfection. LECs were seeded in 6-well plates and grown at 37˚C to 80% confluence. siRELA, or siICAM-1, siSOX18, siPROX1, siFAK, or Negative Control SilencerR No. 1 si-RNA (n.t.Co; 1.75 μg) was mixed with 15 μl Hiperfect transfection reagent (cat. no. 301705; Qiagen GmbH) in 100 μl serum-free EBM2-base medium and left at room temperature to allow formation of transfection complexes for 30 min. Old medium was exchanged for 1.4 ml pre-warmed EBM2-base medium, subsequently transfection-mix was added dropwise to the cells and incubated at 37˚C overnight. On the next day the medium was exchanged for serum containing EGM2-MV medium and cells were left to recover for 24 h.

For the CCID assay, LECs were seeded in 24-well plates and grown at 37˚C to 80% confluence. Subsequently, the EGM2-MV medium was changed to serum free EBM2-base medium and the transfection mix (0.75 μg siRNA; 6 μl Hiperfect transfection reagent; 100 μl serum free medium) was added to the cells and experiments were processed as aforementioned.

12(S)-HETE stimulation. Transfected LECs, which were allowed to recover overnight, were starved in serum free EBM2-base medium at 37˚C for 3 h. Then, LECs were stimulated at 37˚C with 1 μM 12(S)-HETE for 45 min to analyse gene and protein expression using reverse transcription-quantitative (RT-q) PCR and western blot analysis, respectively. Each experiment was performed with three biological replicates.

Western blot analysis. LECs were seeded in 6-well plates and grown at 37˚C to 80% confluence, then 5, 10 and 15 μM Bay11-7082 was added and cells were incubated for 4 h at 37˚C. LECs were then lysed in 2X SDS lysis buffer containing 0.5 M Tris-HCl (pH 6.8), 20% SDS, 10% glycerol, 0.5 M Ethylenediaminetetraacetic acid, phosphatase inhibitor cocktail and protease inhibitor cocktail and sonicated in a pulsed manner using a Branson Sonifier 2000 (Emerson Electric Co.). After centrifugation (12,000 x g; room temperature; 1 min), the supernatant was mixed with 6X loading dye [0.6 M DTT, 24% (w/v) SDS, 36% (v/v) glycine, bromophenol blue, 1.2 M Tris-HCl pH 6.8] and heated for 5 min at 95˚C. Equal amounts of protein (20 μg), as determined by Pierce BCA protein assay (Thermo Fisher Scientific Inc.), were separated using 10% SDS-PAGE (80 V 10 min; 110 V 2 h; constant voltage) using Mini Protean Tetracell (Bio-Rad Laboratories, Inc.) following the manufacturers protocol. Subsequently, proteins were electro-blotted (20 V constant; on ice, overnight) onto Immobilon FL PVDF membrane (0.45 μm pore size; EMD Millipore) using transfer buffer containing 20 mM Tris-base, 150 mM glycine, 20% (v/v) methanol, pH 8.5. Membranes were stained using Ponceau S (Sigma-Aldrich; Merck KGaA) to control transfer efficiency and equal loading. Membranes were blocked at room temperature in 5% dried skim milk in TBS-T (1X Tris buffered saline/0,1% Tween-20; pH 7.6) for 1 h and incubated with either anti-pFAK, anti-FAK, anti-RELA, anti-ICAM-1, anti-SOX18, anti-PROX1 and anti-β-actin antibodies (specified in the subparagraph 'Antibodies and reagents'), agitated at 4˚C, overnight. Then, membranes were washed three times in TBS-T and incubated with HRP-conjugated swine anti-rabbit antibody, or rabbit anti-mouse antibody at room temperature for 1 h. Chemiluminescence was measured using a Lumi-Imager F1 Workstation (Roche Diagnostics) and densitometry was calculated using ImageJ software version 1.51 (National Institutes of Health) and Excel 2013 (Microsoft Corporation). For repetitive analyses, membranes were stripped in between antibody incubations with Restore Western Blot Stripping Buffer (Thermo Fisher Scientific, Inc.) at 37˚C for 5-10 min followed by 3 washes in TBS-T (Sigma-Aldrich; Merck KGaA). Each western blot analysis was performed using three biological replicates.

RT-qPCR. RNA of transfected and stimulated LECs was extracted using RNeasy-Mini-kit and Qia-shredder (both Qiagen GmbH). RNA concentration was measured using a Nano-Drop fluoro-spectrometer (Thermo Fisher Scientific, Inc.) and 2.5 μg RNA were reverse-transcribed using RNA-to-cDNA-EcoDry™ Premix Random Hexamers (Takara Bio Europe SAS) at 42˚C for 60 min and the reaction was stopped at 70˚C for 10 min. Gene expression was analysed using TaqMan Gene Expression Master Mix (Applied Biosystems; Thermo Fisher Scientific, Inc.), TaqMan primers for RELA, ICAM-1, SOX18, PROX1 and β-actin was used as a reference gene, and the CFX 96 Real Time PCR Detection system (Bio-Rad Laboratories, Inc.) and was quantified using the $2^{\Delta\Delta Cq}$ method (23). The thermocycling conditions were as follows: First cycle 50˚C for 2 min, then 1 cycle 95˚C for 10 min, then 40 cycles at 95˚C for 15 sec, 60˚C for 30 sec, 72˚C for 30 sec, and a last cycle at 72˚C for 10 min. Analysis was subsequently performed using three biological replicates.

12(S)-HETE assay. HCT116 cells were seeded in 6-well plates and grown at 37˚C in complete MEM medium to 90% confluence and starved overnight. Cells were then treated with 10 μM arachidonic acid simultaneously with 40 μM proadifen, 40 μM guanfacine, 40 μM vinpocetine or solvent (DMSO) in serum free medium at 37˚C for 4 h. The supernatant (1.5 ml) was collected, butylated hydroxytoulene (0.001% final concentration; cat. no. B1378; Sigma-Aldrich; Merck KGaA) was added to stabilise the secreted eicosanoid, and centrifuged at 280 x g at 4˚C for 5 min. The 12(S)-HETE concentration was determined as described previously (24). Samples were either flash frozen in liquid nitrogen and stored at -80˚C until further analysis or immediately passed through extraction cartridges (Oasis™ HLB 1 cc; Warers Corporation; equilibrated with 2x1 ml methanol, 2x1 ml ddH_2O immediately before use) followed by washing of cartridges with 3x1 ml distilled H_2O. Bound 12(S)-HETE was eluted with 500 μl methanol. After

the evaporation of methanol with an Eppendorf Speedvac Concentrator Plus (Eppendorf) at 30˚C for 2 h, the samples were reconstituted with 100 μl assay buffer of the 12(S)-HETE enzyme immunoassay kit (EIA; cat. no. ADI-900-050; Enzo Life Sciences, Inc.) and subjected to 12(S)-HETE analysis according to the manufacturers protocol (24). Absorbance at 405 nm was measured with a Wallac 1420 Victor 2 multilabel plate reader (PerkinElmer, Inc.). The concentration of 12(S)-HETE in the cellular supernatant was normalised to cell number. The analysis was performed using three biological replicates.

Spheroid formation. Per spheroid, 6000 HCT116 cells were added to MEM medium containing 10% FCS and 0.3% methylcellulose (final concentration) and 150 μl containing 6,000 cells were seeded into each U-bottom shaped well of 96-well plates (Cellstar; cat. no. 650185, Greiner Bio One International GmbH). After centrifugation at 300 x g, room temperature for 15 min, spheroids were grown at 37˚C and 5% CO_2 for two days.

CCID assay. LECs were seeded (20,000 cells/well) in 24-well plates (Costar; cat. no. 3524, Sigma-Aldrich; Merck KGaA) and grown at 37˚C to ~100% confluence. To measure the size of the cell free areas (circular chemorepellent-induced defects; CCIDs), which were formed in the endothelial monolayer directly underneath the tumour spheroids, LECs were stained with CellTracker™ Green CMFDA (Thermo Fisher Scientific, Inc.) at 37˚C for 1 h. For the treatment with 2, 3 and 5 μM curcumin, 5 and 10 μM parthenolide, 2.5 and 5 μM Bay11-7082 and 2.5, 5, 10 and 15 μM defactinib, HCT116 spheroids and LEC monolayers were washed with PBS and pre-incubated with the different concentrations of these compounds in EMB2-base medium at 37˚C for 20 min. The EBM2-base medium including the spheroids and inhibitors was transferred to the LEC monolayers and co-incubated at 37˚C for 4 h. CCID areas in the LEC monolayers were imaged using an Axiovert fluorescence microscope with a magnification of x200 (Zeiss GmbH) using at least 15 fields of view; the size of the areas was calculated with Zen Little 2012 software (Zeiss GmbH). For each condition, the CCIDs in the LEC monolayer underneath at least 15 HCT116-spheroids, which were between ~500-600 μM in diameter and surrounded by a homogenously confluent LEC monolayer, were analysed. The CCID assay was performed using three biological replicates of which at least 5 fields of view were analyzed.

Statistical analysis. Excel 2013 (Microsoft Corporation) software and GraphPad Prism 6 (GraphPad Software, Inc.) were used for one-way ANOVA and unpaired Student's t-test statistics. The data were expressed as mean ± SEM. $P<0.05$ was considered to indicate a statistically significant difference.

Results

12(S)-HETE upregulates RELA and SOX18, which regulate each other in a positive feedback loop. When LECs were stimulated with 12(S)-HETE, the expression of RELA, which is a constituent of the canonical NF-κB transcription factor heterodimer, was induced (Fig. 1A). 12(S)-HETE also induced the expression of SOX18 mRNA and protein in LECs (18) (Figs. S1 and S2). Conversely, the specific inhibition of RELA by siRNA (siRELA; the suppression of RELA at the mRNA and protein levels by siRELA, as opposed to non-target RNA, is shown in Fig. S3 and Fig. 1A, respectively) reduced the expression of SOX18 mRNA (Fig. 1B), as well as that of PROX1, which is a transcriptional target of SOX18 (Fig. 1C). This demonstrated that the constitutive expression of SOX18 and PROX1 were positively regulated by RELA in LECs. It has recently been demonstrated that RELA controls the 12(S)-HETE-stimulated upregulation of SOX18 and PROX1 (18). Since ICAM-1 is an accepted target of the NF-κB transcription factor in ECs (20,25), and specifically of RELA (18), the expression of ICAM-1 mRNA was examined, to control whether the activity of RELA was increased upon 12(S)-HETE-treatment of LECs (18) (Fig. S4). The inhibition of SOX18 by siSOX18 abrogated the 12(S)-HETE-stimulated mRNA upregulation of RELA (Fig. 1D) and ICAM-1 (Fig. 1E). To control whether the SOX18 transcription factor was activated upon 12(S)-HETE treatment of LECs the mRNA expression of its target, PROX1 expression was analysed (Fig. S5; the suppression of SOX18 mRNA- and protein levels by siSOX18, as opposed to non-target RNA, is presented in Figs. S6 and S7, respectively). The data indicated that RELA and SOX18 were positively feeding back to each other in 12(S)-HETE-stimulated LECs (Fig. 1F).

RELA and SOX18 regulate constitutive and 12(S)-HETE-induced FAK phosphorylation. Previous studies have reported that matrix metalloproteinase-1 activated the protein activated receptor 1 and Ca^{2+}-release in LECs, inducing MLC2 and FAK, all of which are prerequisites for their retraction and CCID formation (6,12). In contrast, 12(S)-HETE has been indicated to activate the receptors 12-HETER, BLT2 and Ca^{2+}-release (10,11), as well as the transcription factors NF-κB and SOX18 in LECs (18). NF-κB communicates with FAK in macrophages (26) and, conversely, NF-κB itself is controlled by FAK in endothelial and other types of cells (13,14). Therefore, the current study investigated whether 12(S)-HETE activated FAK in LECs and studied the potential roles of RELA and SOX18 in such a signal transduction pathway. The results revealed that 12(S)-HETE induced the phosphorylation of FAK at tyrosine 397 (Fig. 2A). The transfection of siRELA caused an increase in FAK phosphorylation under constitutive cell culture conditions (Fig. 2A), indicating that RELA suppressed constitutive FAK activity in LECs (Fig. S8). Additionally, 15 μM Bay11-7082 was indicated to induce hyperphosphorylation of FAK and an increase in FAK protein expression, whereas lower Bay11-7082 concentrations (5 and 10 μM) caused a gradual decrease in FAK phosphorylation (Fig. 2B). Bay11-7082 inhibited RELA and the degradation of IκBα, and therefore inhibited the entire panel of NF-κB transcription factors (and possibly also other cellular activities; Fig. 2B). This may have been the reason for the increase in FAK protein expression and for the dose-independent phosphorylation of FAK (Fig. 2B). When RELA was inhibited by siRELA, simultaneous stimulation with 12(S)-HETE did not significantly change the phosphorylation level of FAK, although an additive over-phosphorylation of FAK was hypothetically expected

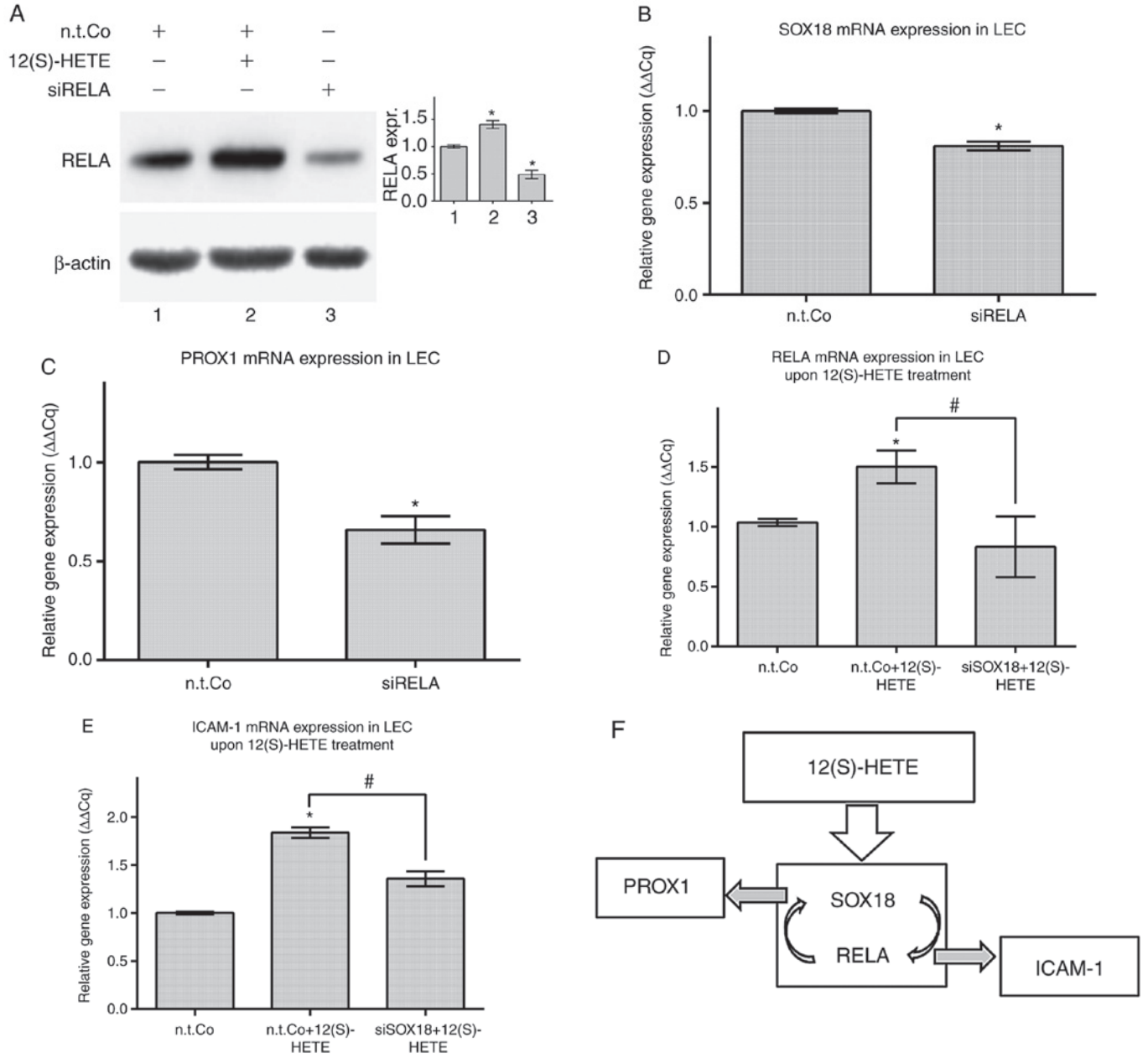

Figure 1. 12(S)-HETE stimulation was shown to upregulate the expression of RELA and ICAM-1. LECs were stimulated with 1 μM 12(S)-HETE for 45 min when (A) protein was isolated for western blot analysis. Ponceau S staining (data not shown) was used, and β-actin expression served as the loading control. Relative protein expression was quantified using densitometry. RELA was indicated to control the expression of SOX18 and PROX1. LECs were transiently transfected with siRNA targeting RELA (siRELA) or non-targeting RNA (n.t.Co) and the mRNA expression of (B) SOX18 and (C) PROX1 was determined using RT-qPCR. SOX18 was shown to control the expression of RELA and ICAM-1. LECs were transiently transfected with siRNA targeting SOX18 (siSOX18) or non-targeting RNA (n.t.Co) and the mRNA expression of (D) RELA and (E) ICAM-1 was determined using RT-qPCR. All experiments were performed in triplicate. Error bars present the ± standard error mean of at least 3 measurements. Statistical significance was determined using ANOVA/Tukey's post hoc test (A, D and E) and t-test (B and C). *P<0.05 vs. n.t.Co. #P<0.05 vs. 12(S)-HETE stimulation. (F) Schematic presentation of the regulation of SOX18, PROX1, RELA and ICAM-1 upon stimulation of LECs with 12(S)-HETE. 12(S)-HETE, 'S' stereoisomer 12S-hydroxy-5Z,8Z,10E,14Z-eicosatetraenoic acid; RELA, v-rel avian reticuloendotheliosis viral oncogene homolog A; LECs, lymph endothelial cells; SOX18, prospero homeobox 1; PROX1, prospero homeobox 1; ICAM-1, intercellular adhesion molecule 1; RT-q, reverse transcription-quantitative; si, small interfering; n.t.Co, non-targeting RNA.

(Fig. 2A). Therefore, it remained unresolved which condition (siRELA-transfection or 12(S)-HETE-stimulation) caused the increase of FAK phosphorylation, as the interpretation of the observed effect was not able to be performed.

Similar to siRELA, siSOX18 also induced the phosphorylation of FAK under constitutive conditions (Fig. 2C), demonstrating an inhibitory effect of SOX18 on FAK activity (Fig. S8). However, in contrast to siRELA, siSOX18 prevented the 12(S)-HETE-triggered phosphorylation of FAK (Fig. 2C). Hence, the RELA/SOX18 circuit suppressed the phosphorylation of FAK under constitutive conditions, whereas the suppressive function of SOX18 on FAK became an activating one when LECs were stimulated with 12(S)-HETE (Fig. 2D).

FAK feeds back to RELA and SOX18. When FAK was inhibited by siFAK transfection (FAK protein suppression is presented in Fig. S9), the 12(S)-HETE-triggered upregulation of RELA and ICAM-1 mRNAs was prevented (Fig. 3A and B,

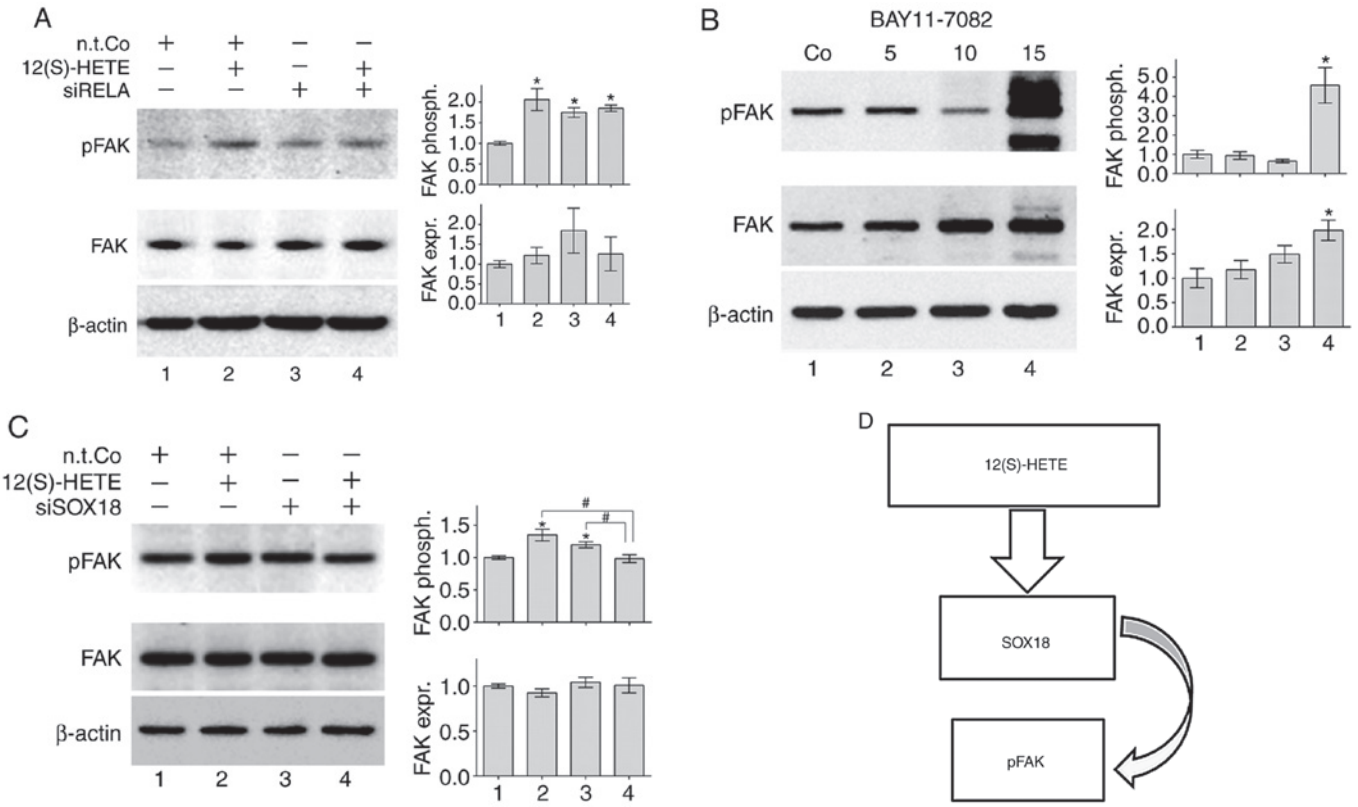

Figure 2. RELA and SOX18 signalling is associated with FAK. (A) LECs were transiently transfected with non-targeting RNA (n.t.Co) or siRNA targeting RELA (siRELA) followed by stimulation with 1 μM 12(S)-HETE for 45 min. (B) LECs were treated with the solvent (DMSO or Co) or with 5-15 μM Bay11-7082 for 4 h. (C) LECs were transiently transfected with non-targeting RNA (n.t.Co) or siRNA targeting SOX18 (siSOX18) followed by stimulation with 1 μM 12(S)-HETE for 45 min. (A-C) Next, the expression of FAK and its phosphorylation at tyrosine 397 was analysed using western blotting. Ponceau S staining (data not shown) was used, and β-actin expression served as the loading control. Relative protein expression was quantified using densitometry. pFAK expression was normalised to respective FAK protein levels. All experiments were performed in triplicate. Error bars present the ± standard error mean of at least 3 measurements. Statistical significance was determined using ANOVA/Tukey's post hoc test (A and C) and ANOVA/Dunnett's post hoc test (B). *P<0.05 vs. n.t.Co. $^{\#}$P<0.05 vs. 12(S)-HETE stimulation. (D) Schematic presentation of SOX18 positively regulating 12(S)-HETE-stimulated phosphorylation of FAK in LECs. RELA, v-rel avian reticuloendotheliosis viral oncogene homolog A; 12(S)-HETE, 'S' stereoisomer 12S-hydroxy-5Z,8Z,10E,14Z-eicosatetraenoic acid; SOX18, prospero homeobox 1; FAK, focal adhesion kinase; LECs, lymph endothelial cells; si, small interfering; p, phosphorylated; n.t.Co, non-targeting RNA.

respectively). Therefore, it can be suggested that FAK positively regulated RELA when LECs were stimulated with 12(S)-HETE (Fig. 3C).

The transfection of siFAK into LECs reduced the constitutive expression of SOX18 mRNA (unlike RELA mRNA) and abolished the 12(S)-HETE-triggered upregulation of SOX18 mRNA (Fig. 3D), such as that of RELA mRNA (Fig. 3A).

Therefore, FAK positively controlled SOX18 expression in 12(S)-HETE-treated and untreated LECs. siFAK inhibited the target of SOX18, PROX1 under constitutive conditions, whereas upon stimulation with 12(S)-HETE, PROX1 was independent of FAK (Fig. 3E). Although SOX18 mRNA was downregulated by siFAK, the SOX18 protein may have been activated by 12(S)-HETE-treatment, thereby inducing the transcription of PROX1. This could explain why PROX1 mRNA (unlike ICAM-1 mRNA) escaped the siFAK-induced downregulation. In conclusion, when LECs were stimulated with 12(S)-HETE, the expression of RELA/SOX18 was induced and positively regulated. Furthermore, the RELA/SOX18 circuit activated FAK, which itself was positively feeding back to SOX18/RELA (Fig. 3F).

Inhibition of lymph endothelial barrier breaching by molecular silencing and pharmacological drugs. The destabilisation of the lymph endothelial barrier due to LEC-retraction is a prerequisite for cancer intra- and extravasation (7), and is a hallmark for the formation of the pre-metastatic niche (27). A trigger of LEC-retraction is 12(S)-HETE, which is secreted by a number of cancer types (7,32). In HCT116 cells, 12(S)-HETE is metabolised by cytochrome P450 1A1 (CYP1A1) from arachidonic acid (28,29) as evidenced by the compromised 12(S)-HETE synthesis through the CYP1A1 inhibitors proadifen, guanfacine and vinpocetine (29-32; Fig. S10). RELA, as the major monomer of the heterodimeric transcription factor NF-κB, regulates the expression of a large number of genes; SOX18 is also known to control the expression of several genes. In order to monitor the pro-intravasative effect of these transcription factors in the CCID assay more specifically, the current study did not knock down RELA and SOX18. Instead, their targets, ICAM-1 and PROX1, were assessed, respectively. These targets were silenced using siRNAs, as they were both reported to attenuate CCID formation, similar to RELA and SOX18 (6,20,18). The specific inhibition of PROX1 or FAK reduced CCID formation by ~25% and the inhibition of ICAM-1 by ~12%. When PROX1 and ICAM-1, or FAK and ICAM-1 were simultaneously inhibited, CCIDs were also reduced, if only by ~25%, similar to the inhibition of PROX1 or FAK alone (Fig. 4A). This suggested that PROX1

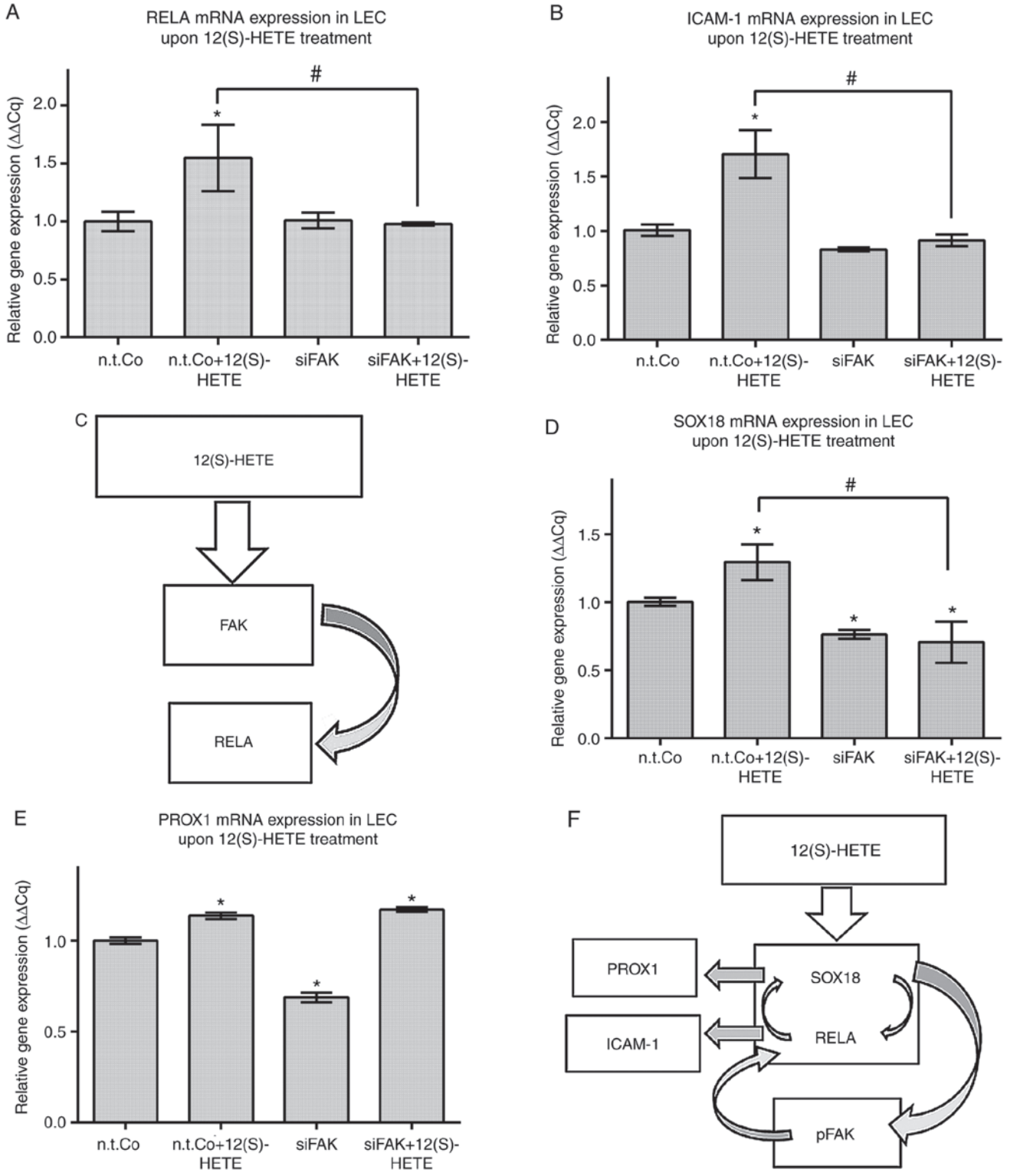

Figure 3. FAK was shown to regulate RELA, ICAM-1 and SOX18 in 12(S)-HETE stimulated cells. LECs were transiently transfected with siRNA targeting FAK (siFAK) or with non-targeting RNA (n.t.Co), stimulated with 1 μM 12(S)-HETE for 45 min and then the mRNA expression of (A) RELA, (B) ICAM-1, (D) SOX18 and (E) PROX1 was analysed by RT-qPCR. All experiments were performed in triplicate. Error bars present the ± standard error mean of at least 3 measurements. Statistical significance was determined by ANOVA/Tukey's post hoc test. *P<0.05 vs. n.t.Co. P<0.05 vs. 12(S)-HETE stimulation. (C and F) Schematic presentations of (C) FAK positively regulating RELA when LECs were stimulated with 12(S)-HETE, and (F) 12(S)-HETE inducing the RELA/SOX18 circuit, which upregulated PROX1 and activated FAK. FAK positively signalled back to RELA, ICAM-1 and SOX18. RELA, v-rel avian reticuloendotheliosis viral oncogene homolog A; ICAM-1, intercellular adhesion molecule 1; SOX18, prospero homeobox 1; 12(S)-HETE, 'S' stereoisomer 12S-hydroxy-5Z,8Z,10E,14Z-eicosatetraenoic acid; LECs, lymph endothelial cells; FAK, focal adhesion kinase; PROX1, prospero homeobox 1; si, small interfering; n.t.Co, non-targeting RNA.

and ICAM-1, as well as FAK and ICAM-1, resided in common pathways involving RELA. The suppression of the protein levels of ICAM-1 by siICAM-1 and of PROX1 by siPROX1, as opposed to non-target RNA, is presented in Figs. S11 and S12.

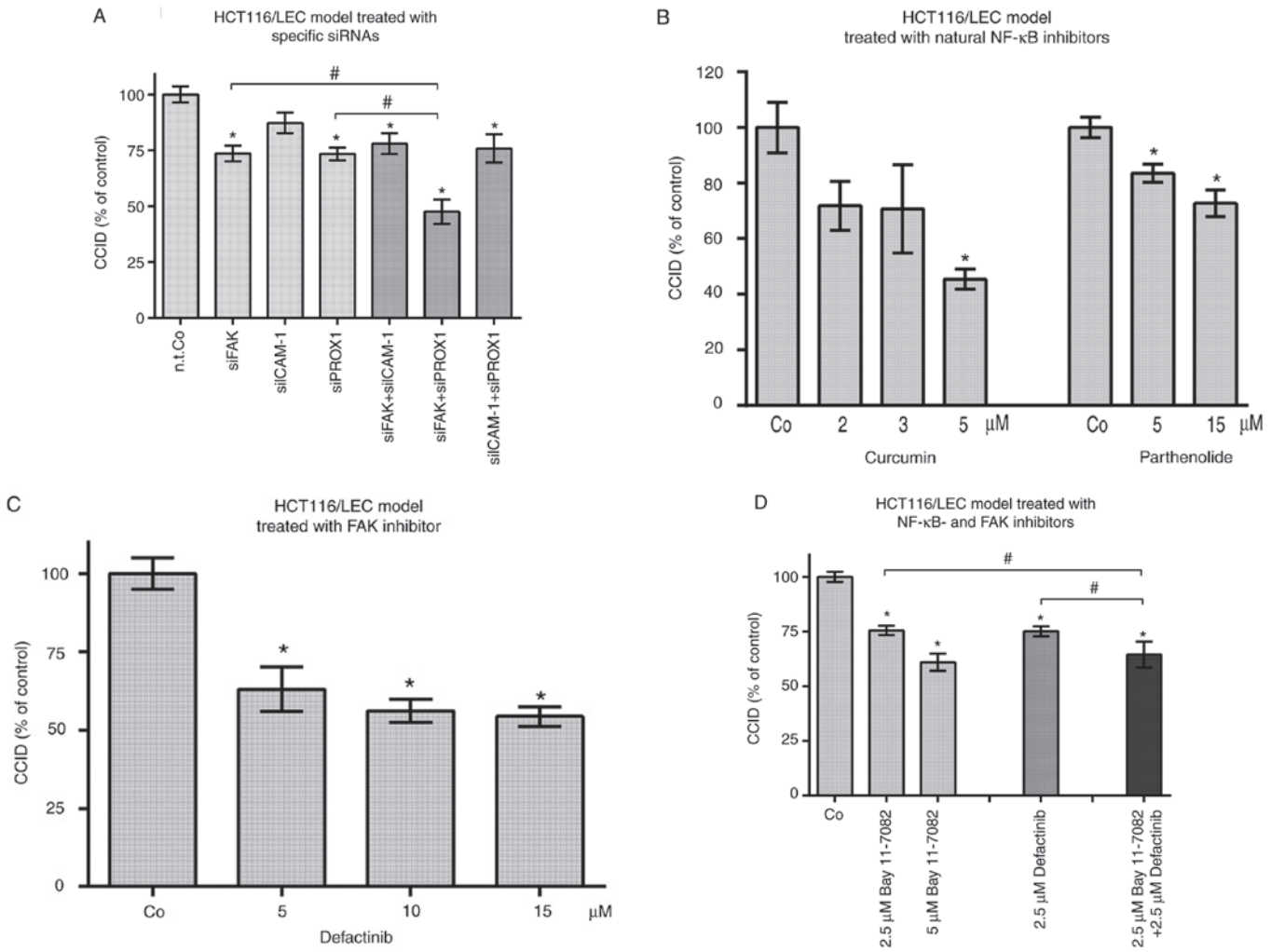

Figure 4. Molecular inhibition of LEC barrier breaching as measured using CCID formation. (A) LECs were transiently transfected with either siRNA alone targeting FAK (siFAK), ICAM-1 (siICAM-1), PROX1 (siPROX1) and non-targeting RNA (n.t.Co), or in the following combinations: siFAK and siICAM-1, siFAK and siPROX1, siICAM-1 and siPROX1. Curcumin, parthenolide, Bay11-7082 and defactinib were shown to inhibit CCID formation. (B-D) LECs were pre-treated with the solvent (DMSO or Co) or the indicated concentrations of (B) curcumin and parthenolide, naturally occurring NF-κB inhibitors, for 20 min, (C and D) defactinib, a FAK inhibitor currently at phase II clinical trial, or (D) the indicated concentrations of Bay 11-7082 alone or in combination with defactinib for 15 min. Experiments were conducted in triplicate analysing at least five spheroids per replicate. Error bars present the ± standard error mean of ≥15 measurements. Statistical significance was determined by ANOVA/Tukey's post hoc test (A and D) and ANOVA/Dunnett's post hoc test (B and C). *P<0.05 vs. n.t.Co or Co. $^{\#}$P<0.05. LEC, lymph endothelial cell; CCID, circular chemorepellent-induced defect; FAK, focal adhesion kinase; ICAM-1, intercellular adhesion molecule 1; PROX1, prospero homeobox 1; si, small interfering; Co, control treatment using DMSO (solvent); n.t.Co, non-targeting RNA.

The suppression of the respective *ICAM-1* and *PROX1* mRNA levels has been demonstrated in previous studies (6,18). The simultaneous inhibition of PROX1 and FAK demonstrated an additive effect and suppressed CCID formation by ~50%, which suggested that PROX1 and FAK were residents of distinct cross-talking pathways. The cross-talking link may have been SOX18, mediating separate signals to FAK and PROX1 (Fig. 3F). SOX18 could therefore have caused endothelial barrier destabilisation via two distinct mechanisms.

siRNA-based approaches are not a treatment option currently. However, natural NF-κB inhibitors are available. Therefore, the HCT116/LEC model was treated with curcumin and parthenolide to inhibit NF-κB (Fig. 4B), or with defactinib to inhibit FAK (Fig. 4C), all of which attenuated CCID formation. As curcumin and parthenolide are likely to inhibit a broad spectrum of molecules in addition to NF-κB, the HCT116/LEC model was also treated with the synthetic and considerably more specific NF-κB inhibitor Bay11-7082 (Fig. 4D). The combination of Bay11-7082 and defactinib attenuated CCID formation additively (Fig. 4D). This suggested that Bay11-7082 may have also inhibited SOX18/PROX1, as a consequence of the RELA/SOX18 circuit, or that defactinib inhibited additional molecules beyond FAK.

Discussion

The aim of the present study was to investigate whether interference with the NF-κB/SOX18/FAK feedback loops may have affected the resilience of the lymph endothelial barrier by measuring the spheroid-induced destabilisation of the LEC monolayer.

FAK is widely associated with the outgrowth, dissemination and colonisation of various tumours at distant sites (33). Cancer cells often travel through blood and lymphatic vessels and reach premetastatic niches, which require the destabilisation and crossing of endothelial walls (4,7,27). The endothelial

barrier-destabilising contribution of FAK, which supports the mobility of LECs, was demonstrated in a previous study (12). In the present study, a formerly unknown signalling network activating FAK upon stimulation of LECs with 12(S)-HETE (an arachidonic acid metabolite), which triggers LEC retraction (8) and CCID formation, is reported, and this was indicated to be a prerequisite for tumour cell intra- and extravasation (7). Due to its involvement in cancer dissemination, FAK has been attracting increasing attention in anti-metastasis research. Currently the effect of the FAK inhibitor defactinib has been tested in 15 clinical trials against a variety of malignancies. Of which, a total of 15 trials were terminated and five were completed, of which one was already at phase II (Clinical Trials. gov Identifier: NCT01951690). However, no results have been published so far. A total of 5 other trials are still recruiting patients currently.

The present data indicated that the activation of FAK upon stimulation of LECs with 12(S)-HETE was regulated by SOX18 and RELA. RELA and SOX18 were positively feeding-back to each other and also influenced the expression of the partner targets (RELA influenced SOX18 and PROX1 and SOX18 influenced RELA and ICAM-1). As has been previously reported, SOX18 and NF-κB are associated with eachother (17,18) and NF-κB was demonstrated to regulate the expression of FAK (26). These observations were consistent with the data of the current study.

FAK was also indicated to feed back to RELA, ICAM-1 and SOX18 but not to PROX1, suggesting that the signal triggered by 12(S)-HETE arrived at RELA before it activated the other components. RELA and SOX18 are transcription factors without a known kinase function. Therefore, the phosphorylation of FAK must be associated with tyrosine kinases or phosphatases when cells were treated with 12(S)-HETE under constitutive conditions, respectively. FAK tyrosine 397 becomes cis- or trans-autophosphorylated (34) when FAK is associated with integrin-beta subunits. The upregulation of integrin αvβ3 was demonstrated to depend on NF-κB, leading to the activation of FAK and increased the motility of human lung cancer cells (35). Integrins also become activated when in contact with transcriptional targets of NF-κB, including vimentin (36). Alternatively, NF-κB activates FAK in LECs through the upregulation of interleukins (IL; including IL-6), which causes the recruitment of Src at the Src Homology 2 (SH-2) and SH-3 domains of FAK in LECs (37). In turn, Src itself and other Src-family kinases, including Fyn and Yes have been indicated to phosphorylate tyrosine 397 (38,39). Conversely, this residue is dephosphorylated by the SH2 domain containing protein-tyrosine phosphatase 2 (SHP-2) in ECs, which stabilises vascular permeability (40), and SHP-2 is regulated by NF-κB (41). Hence, SHP-2, Src, vimentin and integrins might have been involved in NF-κB-dependent constitutive- or 12(S)-HETE-induced phosphorylation of FAK tyrosine 397.

SOX18, which inhibited FAK activity under constitutive conditions, became an activator of FAK upon stimulation with 12(S)-HETE. Physiologically, 12(S)-HETE and other molecules are secreted by neutrophils and macrophages, which enable their passage through lymph endothelial barriers and into the adjacent stroma (9). In this scenario, the regulatory function of NF-κB/RELA helps combat infections. Pathologically, tumour-secreted 12(S)-HETE unlocks the lymph endothelial cell wall, and in this scenario, RELA supports malignant dissemination. Therefore, an immune cell-specific mechanism, which is required to reach various types of body tissues, becomes re-activated in cancer cells. It has previously been demonstrated that 12(S)-HETE causes the disintegration of endothelial barriers by inducing endothelial-to-mesenchymal transition (endo-MT) (19,42). In molecular terms, 12(S)-HETE has been revealed to upregulate S100A4, ZEB1 and the mobility proteins MCL2 and myosin phosphatase target, and to transiently downregulate vascular endothelial-cadherin in ECs (7,11,20). These polypeptides, which are tightly linked to endo-MT and cause endothelial retraction, also facilitate the formation of pre-metastatic niche (PMN) (43,44). Other authors have provided evidence that activated FAK contributes to the formation of PMN at distant sites in pancreatic (45) and breast (46) cancer, which is based on the reduced endothelial barrier function adjacent to the pre-metastatic organ. This is not only a hallmark of PMN (27), but also indicative for endo-MT (12,19). In support of this observation, the siRNA-mediated suppression of FAK was shown to inhibit the haptotaxis/haptokinesis (directional migration) of pancreatic carcinoma cells (47), as well as directional endothelial cell migration that was triggered by breast cancer cell spheroids (12). Therefore, 12(S)-HETE fulfils the criteria of an endo-MT trigger factor (19,27) and might therefore contribute to the formation of the PMN at a very early step of metastatic dissemination. Targeting crucial signalling pathways might attenuate the metastatic process. The current study demonstrated that RELA, SOX18 and FAK were integrated in a signalling network when LECs were stimulated with 12(S)-HETE. As both NF-κB and FAK are common signal transducers for various cell functions in several cell types, the specificity is marginal and the toxic side effects are probably substantial. However, as this pro-metastatic mechanism also involved SOX18 and its target PROX1 (18), both transcription factors are specific for endothelial development and lymph endothelial maintenance (15,16), therefore, identifying specific inhibitors that target these polypeptides is required. Inhibitors of SOX18, and eventually PROX1, may reduce non-specific toxicity and exert improved anti-metastatic effects by strengthening the resilience of the lymphatic barrier and attenuating the voyage of cancer cells through the lymphatic route.

Acknowledgements

The authors would like to thank Dr Adryan Fristiohady (Faculty of Pharmacy, Halu Oleo University, Kendari, Indonesia) for helping to train the masters student Stefanie Engleitner, and the authors would also like to thank Mr. Toni Jäger, Department of Pathology, Medical University of Vienna, for preparing the figures.

Funding

JH was supported by a State Scholarship Fund of China Scholarship Council, the National Natural Science Foundation of China (grant no. 81202853), the Natural Science Foundation of Jiangsu Province (grant no. BK2012444) and Jiangsu

Planned Projects for Postdoctoral Research Funds. AF was supported by a DIKTI-OeAD fellowship, and CHN by a technology grant (TSA Doktorat) financed by the Austria Federal Ministry of Science and Research (BMFW) in frame of Asea Uninet. GK was supported by the Austrian Science Fund (FWF)/Herzfelder'sche Familienstiftung (project no. P 30572-B28 and ZB-H) by a grant of the Medical Scientific Funds of the Mayor of the City of Vienna (grant no. 15116).

Availability of data and materials

The datasets used and/or analyzed during the current study are available from the corresponding author on reasonable request.

Authors' contributions

GK, RDM, WJ, ZBH conceptualized the current study. GK, WJ, RDM, DM and SK designed the current study. SE, DM, KK, SB, JH and NR acquired the data. GK, NH, JR and CHN performed quality control of the data and algorithms. SE, WJ, RDM and GK analyzed and interpreted the data. SE, DM and KK performed statistical analysis. GK, SE, RDM and WJ prepared the manuscript. SE, ZBH, SK, GK, RDM and WJ edited the manuscript. All authors read and approved the final manuscript.

Ethics approval and consent to participate

Not applicable.

Patients consent for publication

Not applicable.

Competing interests

The authors declare that they have no competing interests.

References

1. Paget S: The distribution of secondary growth in cancer of the breast. Lancet 1: 99-101, 1889.
2. Fidler IJ: The pathogenesis of cancer metastasis: The 'seed and soil' hypothesis revisited. Nat Rev Cancer 3: 453-458, 2003.
3. Nguyen DX, Bos PD and Massagué J: Metastasis: From dissemination to organ-specific colonization. Nat Rev Cancer 9: 274-284, 2009.
4. Reymond N, d'Água BB and Ridley AJ: Crossing the endothelial barrier during metastasis. Nat Rev Cancer 13: 858-870, 2013.
5. Uchide K, Sakon M, Ariyoshi H, Nakamori S, Tokunaga M and Monden M: Cancer cells cause vascular endothelial cell (vEC) retraction via 12(S)HETE secretion; the possible role of cancer cell derived microparticle. Ann Surg Oncol 14: 862-868, 2007.
6. Nguyen CH, Senfter D, Basilio J, Holzner S, Stadler S, Krieger S, Huttary N, Milovanovic D, Viola K, Simonitsch-Klupp I, *et al*: NF-κB contributes to MMP1 expression in breast cancer spheroids causing paracrine PAR1 activation and disintegrations in the lymph endothelial barrier in vitro. Oncotarget 6: 39262-39275, 2015.
7. Kerjaschki D, Bago-Horvath Z, Rudas M, Sexl V, Schneckenleithner C, Wolbank S, Bartel G, Krieger S, Kalt R, Hantusch B, *et al*: Lipoxygenase mediates invasion of intrametastatic lymphatic vessels and propagates lymph node metastasis of human mammary carcinoma xenografts in mouse. J Clin Invest 121: 2000-2012, 2011.
8. Honn KV, Tang DG, Grossi I, Duniec ZM, Timar J, Renaud C, Leithauser M, Blair I, Johnson CR, Diglio CA, *et al*: Tumor cell-derived 12(S)-hydroxyeicosatetraenoic acid induces microvascular endothelial cell retraction. Cancer Res 54: 565-574, 1994.
9. Rigby DA, Ferguson DJ, Johnson LA and Jackson DG: Neutrophils rapidly transit inflamed lymphatic vessel endothelium via integrin-dependent proteolysis and lipoxin-induced junctional retraction. J Leukoc Biol 98: 897-912, 2015.
10. Nguyen CH, Brenner S, Huttary N, Li Y, Atanasov AG, Dirsch VM, Holzner S, Stadler S, Riha J, Krieger S, *et al*: 12(S)-HETE increases intracellular Ca(2+) in lymph-endothelial cells disrupting their barrier function in vitro; stabilization by clinical drugs impairing calcium supply. Cancer Lett 380: 174-183, 2016.
11. Nguyen CH, Stadler S, Brenner S, Huttary N, Krieger S, Jäger W, Dolznig H and Krupitza G: Cancer cell-derived 12(S)-HETE signals via 12-HETE receptor, RHO, ROCK and MLC2 to induce lymph endothelial barrier breaching. Br J Cancer 115: 364-370, 2016.
12. Hong J, Fristiohady A, Nguyen CH, Milovanovic D, Huttary N, Krieger S, Hong J, Geleff S, Birner P, Jäger W, *et al*: Apigenin and luteolin attenuate the breaching of MDA-MB231 breast cancer spheroids through the lymph endothelial barrier in vitro. Front Pharmacol 9: 220, 2018.
13. Dwyer SF, Gao L and Gelman IH: Identification of novel focal adhesion kinase substrates: Role for FAK in NFB signaling. Int J Biol Sci 11: 404-410, 2015.
14. Tavora B, Reynolds LE, Batista S, Demircioglu F, Fernandez I, Lechertier T, Lees DM, Wong PP, Alexopoulou A, Elia G, *et al*: Endothelial-cell FAK targeting sensitizes tumours to DNA-damaging therapy. Nature 514: 112-116, 2014.
15. Kanki Y, Nakaki R, Shimamura T, Matsunaga T, Yamamizu K, Katayama S, Suehiro JI, Osawa T, Aburatani H, Kodama T, *et al*: Dynamically and epigenetically coordinated GATA/ETS/SOX transcription factor expression is indispensable for endothelial cell differentiation. Nucleic Acids Res 45: 4344-4358, 2017.
16. François M, Caprini A, Hosking B, Orsenigo F, Wilhelm D, Browne C, Paavonen K, Karnezis T, Shayan R, Downes M, *et al*: Sox18 induces development of the lymphatic vasculature in mice. Nature 456: 643-647, 2008.
17. Basilio J, Hoeth M, Holper-Schichl YM, Resch U, Mayer H, Hofer-Warbinek R and de Martin R: TNFα-induced down-regulation of Sox18 in endothelial cells is dependent on NF-κB. Biochem Biophys Res Commun 442: 221-226, 2013.
18. Fristiohady A, Milovanovic D, Krieger S, Basilio J, Jäger W, de Martin R and Krupitza G: 12(S)-HETE induces lymphendothelial cell retraction in vitro through contribution of SOX18 and PROX1. Int J Oncol 50: 307-316, 2018.
19. Vonach C, Viola K, Giessrigl B, Huttary N, Raab I, Kalt R, Krieger S, Vo TP, Madlener S, Bauer S, *et al*: NF-κB mediates the 12(S)-HETE-induced endothelial to mesenchymal transition of lymphendothelial cells during the intravasation of breast carcinoma cells. Br J Cancer 105: 263-271, 2011.
20. Viola K, Kopf S, Huttary N, Vonach C, Kretschy N, Teichmann M, Giessrigl B, Raab I, Stary S, Krieger S, *et al*: Bay11-7082 inhibits the disintegration of the lymphendothelial barrier triggered by MCF-7 breast cancer spheroids; The role of ICAM-1 and adhesion. Br J Cancer 108: 564-569, 2013.
21. Yang J, Chang E, Cherry AM, Bangs CD, Oei Y, Bodnar A, Bronstein A, Chiu CP and Herron GS: Human endothelial cell life extension by telomerase expression. J Biol Chem 274: 26141-26148, 1999.
22. Schoppmann SF, Soleiman A, Kalt R, Okubo Y, Benisch C, Nagavarapu U, Herron GS and Geleff S: Telomerase-immortalized lymphatic and blood vessel endothelial cells are functionally stable and retain their lineage specificity. Microcirculation 11: 261-269, 2004.
23. Livak KJ and Schmittgen TD: Analysis of relative gene expression data using real-time quantitative PCR and the 2(-Delta Delta C(T)) method. Methods 25: 402-408, 2001.
24. Stadler S, Nguyen CH, Schachner H, Milovanovic D, Holzner S, Brenner S, Eichsteininger J, Stadler M, Senfter D, Krenn L, *et al*: Colon cancer cell-derived 12(S)-HETE induces the retraction of cancer-associated fibroblast via MLC2, RHO/ROCK and Ca^{2+} signalling. Cell Mol Life Sci 74: 1907-1921, 2017.
25. Zhong L, Simard MJ and Huot J: Endothelial microRNAs regulating the NF-κB pathway and cell adhesion molecules during inflammation. FASEB J 32: 4070-4084, 2018.

26. Wang H, Wang X, Li X, Fan Y, Li G, Guo C, Zhu F, Zhang L and Shi Y: CD68(+)HLA-DR(+) M1-like macrophages promote motility of HCC cells via NF-κB/FAK pathway. Cancer Lett 345: 91-99, 2014.
27. Peinado H, Zhang H, Matei IR, Costa-Silva B, Hoshino A, Rodrigues G, Psaila B, Kaplan RN, Bromberg JF, Kang Y, *et al*: Pre-metastatic niches: Organ-specific homes for metastases. Nat Rev Cancer 17: 302-317, 2017.
28. Zapletal O, Tylichová Z, Neča J, Kohoutek J, Machala M, Milcová A, Pokorná M, Topinka J, Moyer MP, Hofmanová J, *et al*: Butyrate alters expression of cytochrome P450 1A1 and metabolism of benzo[a]pyrene via its histone deacetylase activity in colon epithelial cell models. Arch Toxicol 91: 2135-2150, 2017.
29. Nguyen CH, Brenner S, Huttary N, Atanasov AG, Dirsch VM, Chatuphonprasert W, Holzner S, Stadler S, Riha J, Krieger S, *et al*: AHR/CYP1A1 interplay triggers lymphatic barrier breaching in breast cancer spheroids by inducing 12(S)-HETE synthesis. Hum Mol Genet 25: 5006-5016, 2016.
30. Taira Z, Yamase D and Ueda Y: A new technique for assaying cytochrome P450 enzyme activity in a single cell. Cell Biol Toxicol 23: 143-151, 2007.
31. Teichmann M, Kretschy N, Kopf S, Jarukamjorn K, Atanasov AG, Viola K, Giessrigl B, Saiko P, Szekeres T, Mikulits W, *et al*: Inhibition of tumour spheroid-induced prometastatic intravasation gates in the lymph endothelial cell barrier by carbamazepine: Drug testing in a 3D model. Arch Toxicol 88: 691-699, 2014.
32. Holzner S, Brenner S, Atanasov AG, Senfter D, Stadler S, Nguyen CH, Fristiohady A, Milovanovic D, Huttary N, Krieger S, *et al*: Intravasation of SW620 colon cancer cell spheroids through the blood endothelial barrier is inhibited by clinical drugs and flavonoids in vitro. Food Chem Toxicol 111: 114-124, 2018.
33. Cooper J and Giancotti FG: Integrin signaling in cancer: Mechanotransduction, stemness, epithelial plasticity, and therapeutic resistance. Cancer Cell 35: 347-367, 2019.
34. Hanks SK, Ryzhova L, Shin NY and Brábek J: Focal adhesion kinase signaling activities and their implications in the control of cell survival and motility. Front Biosci 8: d982-d996, 2003.
35. Zhu J, Luo J, Li Y, Jia M, Wang Y, Huang Y and Ke S: HMGB1 induces human non-small cell lung cancer cell motility by activating integrin αvβ3/FAK through TLR4/NF-κB signaling pathway. Biochem Biophys Res Commun 480: 522-527, 2016.
36. Lilienbaum A, Duc Dodon M, Alexandre C, Gazzolo L and Paulin D: Effect of human T-cell leukemia virus type I tax protein on activation of the human vimentin gene. J Virol 64: 256-263, 1990.
37. Huang YH, Yang HY, Huang SW, Ou G, Hsu YF and Hsu MJ: Interleukin-6 induces vascular endothelial growth factor-C expression via Src-FAK-STAT3 signaling in lymphatic endothelial cells. PLoS One 11: e0158839, 2016.
38. Calalb MB, Polte TR and Hanks SK: Tyrosine phosphorylation of focal adhesion kinase at sites in the catalytic domain regulates kinase activity: A role for Src family kinases. Mol Cell Biol 15: 954-963, 1995.
39. Klinghoffer RA, Sachsenmaier C, Cooper JA and Soriano P: Src family kinases are required for integrin but not PDGFR signal transduction. EMBO J 18: 2459-2471, 1999.
40. Chichger H, Braza J, Duong H and Harrington EO: SH2 domain-containing protein tyrosine phosphatase 2 and focal adhesion kinase protein interactions regulate pulmonary endothelium barrier function. Am J Respir Cell Mol Biol 52: 695-707, 2015.
41. Kang HJ, Chung DH, Sung CO, Yoo SH, Yu E, Kim N, Lee SH, Song JY, Kim CJ and Choi J: SHP2 is induced by the HBx-NF-κB pathway and contributes to fibrosis during human early hepatocellular carcinoma development. Oncotarget 8: 27263-27276, 2017.
42. Senfter D, Holzner S, Kalipciyan M, Staribacher A, Walzl A, Huttary N, Krieger S, Brenner S, Jäger W, Krupitza G, *et al*: Loss of miR-200 family in 5-fluorouracil resistant colon cancer drives lymphendothelial invasiveness in vitro. Hum Mol Genet 24: 3689-3698, 2015.
43. Kaplan RN, Riba RD, Zacharoulis S, Bramley AH, Vincent L, Costa C, MacDonald DD, Jin DK, Shido K, Kerns SA, *et al*: VEGFR1-positive haematopoietic bone marrow progenitors initiate the pre-metastatic niche. Nature 438: 820-827, 2005.
44. Kaplan RN, Psaila B and Lyden D: Bone marrow cells in the 'pre-metastatic niche': Within bone and beyond. Cancer Metastasis Rev 25: 521-529, 2006.
45. Houg DS and Bijlsma MF: The hepatic pre-metastatic niche in pancreatic ductal adenocarcinoma. Mol Cancer 17: 95, 2018.
46. Hiratsuka S, Goel S, Kamoun WS, Maru Y, Fukumura D, Duda DG and Jain RK: Endothelial focal adhesion kinase mediates cancer cell homing to discrete regions of the lungs via E-selectin upregulation. Proc Natl Acad Sci U S A 108: 3725-3730, 2011.
47. Lu J, Zhou S, Siech M, Habisch H, Seufferlein T and Bachem MG: Pancreatic stellate cells promote hapto-migration of cancer cells through collagen I-mediated signalling pathway. Br J Cancer 110: 409-420, 2014.